By acceptance of this article, the publisher or recipient acknowledges the U.S. Government's right to retain a nonexclusive, royalty-free license in and to any copyright covering the article.

MASTER

CONF-780811--25

NOTICE
This report was prepared as an account of work sponsored by the United States Government. Neither the United States nor the United States Department of Energy, nor any of their employees, nor any of their contractors, subcontractors, or their employees, makes any warranty, express or implied, or assumes any legal liability or responsibility for the accuracy, completeness or usefulness of any information, apparatus, product or process disclosed, or represents that its use would not infringe privately owned rights.

TOKAMAK DISCHARGE MODELING THROUGH MAGNETIC PERTURBATION EFFECTS: RAPPORTEURING OF PAPERS F-1-1, F-1-2 and F-1-3 *

J. D. Callen
Oak Ridge National Laboratory, Oak Ridge, Tennessee 37830 U.S.A.

In this talk I will be acting as rapporteur for three papers that are basically concerned with tokamak discharge modeling through magnetic perturbation effects.

MASTER

SLIDE #1

The first of the three papers is F-1-1, "Magnetic Islandography in Tokamaks," by an Oak Ridge group, that includes me. The topics discussed in this paper are how: internal disruptions arise from the lowest order (m/n = 1) helical tearing modes; Mirnov Oscillations arise due to m/n = 2 modes, 2/1-3/2 coupling leads to a disruptive instability, and finally a brief discussion of how anomalous transport may come about because of the magnetic perturbations due to microinstabilities.

The next paper (F-1-2) is a paper by Mirnov on "Scaling Laws for Energy Lifetimes in Tokamaks." The basic point of the paper is to develop a universal scaling law of the energy containment time versus q, with q measured however at the edge of the current channel, and trying to determine the degree of correlation with Mirnov Oscillations. The paper shows that the optimum energy containment time occurs for plasmas that are most free of Mirnov Oscillations. This paper arrives at a more or less universal scaling law of the form shown which is in fact, with the addition of the $\sqrt{n_e}$, the same as the old T-3 scaling law.

Finally the last paper in this sequence, F-1-3, is the paper by Dnestrovskii et al., on the "Simulation of Discharge Dynamics in Tokamaks" which concerns two topics. One is the skin current relaxation during the current initiation phase of tokamak discharges that is shown to come about through magnetic reconnection.

DISTRIBUTION OF THIS DOCUMENT IS UNLIMITED

* Research sponsored by the Office of Fusion Energy (ETM), U.S. Department of Energy under contract W-7405-eng-26 with the Union Carbide Corporation.

The second topic in this paper concerns neutral beam heating calculations for T-11.

Except for the last topic, these papers have a common theme -- namely the modeling of tokamak discharge behavior through magnetic perturbation effects. Since this last topic is somewhat different, I will discuss it first.

SLIDE #2 (500 KW NEUTRAL BEAM HEATING IN T-11)

The paper by Dnestrovskii et al. presents calculations illustrating the effects of 500 kw of neutral beam heating in T-11. The basic point shown here is that the electron and ion temperatures are predicted to increase with neutral beam injection in T-11, up to about 1 keV. The authors feel that T-11 may be able to get into the collisionless ($\nu_{*_i} < 1$) or banana regime if the impurity level can be kept low enough ($Z_{eff} < 4$-5) and if the neutral density can be kept low enough -- below about 10^{10} cm^{-3}.

SLIDE #3 (NONLINEAR EVOLUTION OF MAGNETIC PERTURBATIONS)

We will now proceed to discuss the nonlinear effects of magnetic perturbations. Since the three papers are complementary in their discussion of the magnetic perturbation effects on transport, we will discuss them in an integrated fashion, rather than sequentially. On each slide we have indicated in the lower right hand corner the paper from which this slide comes and/or where further information may be obtained. Before going through the various particular modes, I would like to discuss roughly how the magnetic perturbation effects develop, affect the magnetic geometry, nonlinearly evolve, and ultimately affect transport in a tokamak.

We begin with a helically resonant magnetic perturbation or perturbations. Any single one of these produces a magnetic island of helical symmetry. This magnetic island can, in the case of m = 1 modes, lead to a topological flip or magnetic reconnection which then leads to sort of a transport short circuit over the reconnected region.

On the other hand, these magnetic islands can nonlinearly saturate in a steady state. This is what happens in the Mirnov Oscillations which are due to m = 2 modes. These modes also produce as a transport effect a sort of short circuit over the island region.

If there is not just one significant magnetic perturbation, but rather 2 or more magnetic islands of different helicity, then as they grow up to invade each other, that is overlap, they destroy the magnetic flux surfaces in the region where they overlap and this leads to a very rapid transport of heat over the stochastic region. This, in fact is the Oak Ridge model of the disruptive instability.

We will now go on to discuss specific cases of the magnetic perturbations from the lowest mode number m = 1 upward, with emphasis on the transport effects and the degree to which the theory correlates with experiment.

SLIDE #4 (m/n = 1 -- INTERNAL DISRUPTIONS)

The m = 1 mode leads to an internal disruption. Basically what happens is that one begins with an m = 1 tearing mode around the q = 1 surface. This grows as a function of time during the growth of the electron temperature at the plasma center and causes the temperature profile to become flattened in the region around the singular surface. At time t_2 one observes that what was the center of the island has become the center of the plasma and what was the center of the plasma has become in fact a small oddity on the side which will be erased very shortly. Thus there has been what one might call a topological flip. This model of slow resistive heating followed by a topological flip agrees with ORMAK data in: 1) the space time evolution of the m = 1 precursors, which indicates the presence of the island because the plasma is spinning; and 2) with the spatial structure of the internal disruption phenomenon, which is not shown here.

Finally, this understanding of the internal disruption is useful to provide a basis for looking at the heat pulse propagation produced by taking a certain amount of heat from the center and effectively moving it outward. An examination of the space time evolution of this initially nonequilibrium situation allows us to examine the microscopic diffusive transport processes in tokamaks.

SLIDE #5 (ELECTRON HEAT TRANSPORT DETERMINATION)

Examining the space-time evolution of the electron temperature profile it has been found that the electron heat transport determined from that heat pulse propagation is diffusive and microscopic, i.e., on scale lengths <1-2 cm. With more refined analysis than those used originally in this work as reported in Physical Review etters, we now find the same heat conduction coefficient as that of the background plasma. This is shown in the figure with χ_{HPP} denoting the original estimate. The data points shown were derived from the more recent and refined estimate, and compare favorably with the curves of χ_e determined from energy balance calculations in the plasma, with and without radiation effects, that come from the Berchesgarten IAEA paper by Berry et al., on ORMAK data.

SLIDE #6 (m/n = 2 -- MIRNOV OSCILLATIONS)

The next higher mode number is the m/n = 2 mode in the next slide, the energy

The next higher mode number is the m/n = 2 mode which we will now discuss. Here we will be discussing Mirnov Oscillations. To show that that is indeed the case, we will make a very detailed correlation of theory and experiment.

The nonlinear evolution of the m = 2 mode in the high-S regime is given by this equation. That is, the island width grows linearly with $\Delta'(w)$, where w is the island width.

The quasi-linear saturation is observed either from this criterion, or from the non-linear code evaluations, to occur whenever Δ', when evaluated in the presence of the island, vanishes. This then leads to a given maximum island

width, and knowing the eigenfunction one can in fact predict the magnitude of the perturbation $\tilde{B}_\theta$ that should be seen at the loop outside of the plasma.

We will show that the theoretical prediction of this magnetic perturbation level compares favorably with at least ORMAK and T-4 data.

SLIDE #7 (THEORETICAL MIRNOV OSCILLATION AMPLITUDE PEAK AT $q(a) \lesssim 3$)

In this slide we show theoretical estimates for the island width and magnetic perturbation level for m = 2 modes for a variety of relevant current profiles. The basic point illustrated here is that at high q the fluctuation levels are relatively low, the singular surface is relatively deep inside the plasma, and the island widths are small. One obtains the maximum island width and magnetic perturbation level at a q limiter of about 3. The modes become totally stabilized with q less than about 2 because the singular surface is then outside the plasma. Notice that the $\tilde{B}_\theta$ perturbation level is predicted theoretically to vanish even before one actually reaches q = 2. From the insert showing the relevant current profiles we see that the maximum Mirnov oscillation amplitude is very sensitive to the nature of the current profile near the q = 2 singular surface.

SLIDE #8 (THEORETICAL AMPLITUDE AGREES WITH ORMAK DATA)

For exact ORMAK profiles, one finds very good agreement between the experimentally measured $\tilde{B}_\theta$ in ORMAK, which are shown by open circles, and the theoretical calculations shown by dark dots. The temperature profiles are different for each value of q(a). In this sequence of experiments the Mirnov oscillation amplitude is not observed to decrease, as theoretically predicted, at low q. However, similar data for T-4, which also shows a good correlation between theory and experiment, does exhibit a diminished amplitude at low q. As most prominently noted by Mirnov in his paper F-1-2, and as I will discuss further in the next slide, the energy containment time is anticorrelated with the magnitude of the Mirnov oscillations.

That is, when the Mirnov oscillations become large, the energy containment time drops.

SLIDE #9 (ENERGY CONTAINMENT TIME)

The correlation between the Mirnov oscillation amplitude and the energy containment time is exhibited in Mirnov's paper with this slide. Here, he shows in case II the ORMAK data which was referred to on the preceding sslide and in case I some T-4 data. The basic point is that they both exhibit the same general scaling characteristics. However, one notes that the energy containment time peaks at different values of the limiter q in the two different cases.

SLIDE #10 (MIRNOV RECONCILES DIFFERENCE)

Mirnov reconciles this difference in the location of the peak by taking account of the size of the currentless cold plasma mantle or edge region around the plasma. He suggests that the current channel radius (the real current carrying region of the plasma) should be determined by either one of two things: 1) the mean radius of the resonant surface determined from assuming all the current flows within the q = 2 surface; or 2) from the electron temperature profile by saying that when the temperature drops to 1/10 of the central value one has reached the cold edge of the plasma. Either of these is shown to give roughly the same answer for the effective radius a_I of the current carrying region.

The thickness of the currentless cold plasma region is then given by the difference between the limiter radius and the q = 2 radiu . This is governed by experimental conditions, that is to say impurity influx, gas puffing, etc.

What Mirnov then argues is that the relevant q against which the energy containment should be plotted is that at the current channel radius -- that is to say against q at the current channel radius, which is related to the q at the limiter by the quadratic relationship shown.

SLIDE #11 (RENORMALIZING THE q AXIS)

When Mirnov then plots, for a large number of devices, the normalized energy containment time versus q at the current channel radius, he finds a universal scaling curve of the energy containment time versus q at the current channel radius, with the optimum q at the current channel radius being at about 2. The main point which is emphasized in this paper by Mirnov is that in making scaling laws people usually do not take account of the fact that there is a significant variation of the energy containment time with q. In fact, the low-q region represents a region where there is a significant deterioration of containment.

SLIDE #12 (T-3 SCALING LAW)

With this point in mind, he reanalyzes a large amount of the tokamak confinement scaling data. In particular, he includes only those data for which the discharge is effectively stable -- that is the Mirnov oscillations are very small and thus there is not a significant deterioration of the confinement due to the Mirnov oscillations. Doing this he finds that the old T-3 scaling law fits tokamak data better than the Alcator scaling law which he observes probably includes a number of these "unstable" discharges for which there is significant Mirnov oscillation effects. The figure shows the energy containment time derived from the T-3 scaling law (open points) and Alcator scaling law (solid points) versus the experimentally observed value as plotted on the ordinate. The basic points he makes are first that there is less scatter with the T-3 scaling law and second that it in fact predicts the data more closely than the Alcator scaling law.

SLIDE #13 (CONFINEMENT DETERIORATES)

To illustrate specifically the deterioration of the confinement for "unstable" discharges, Mirnov also plots the experimentally measured energy containment time, normalized to his scaling law and hence his prediction of the best confinement,

as a function of q at the current channel radius, for ATC, ORMAK and TFR. What he shows is that in each case there is a deterioration of the confinement as q approaches 2 or 3. Then, in some cases, as would be theoretically predicted, as one gets down very close to 2, the Mirnov oscillations begin to go away and one can perhaps slide into as good as confinement regime as one has at large q.

SLIDE #14 (PLASMA CONFINEMENT DETERIORATES DUE TO ISLAND)

Plasma confinement deteriorates at low q due to the Mirnov induced magnetic islands. To demonstrate this we have calculated transport in a helical flux surface geometry, as shown here for the m = 2 oscillations.

What we find is that one must be careful to realize that while heat is diffusing out from the center of the plasma things change when one comes to an island. If one deposits heat in the center of the island it in fact moves radially outward in both directions from the center of the island. The introduction of a magnetic island leads effectively to a heat flux continuity condition which is such that the heat flux coming to the outside must be the sum of the heat flux coming out from the center of the plasma to the inner edge of the island and the heat deposited in the island. Effectively this leads to a short circuiting of the confinement properties in the region occupied by the island.

For a simple estimate one can calculate the effect of the presence of this island on the energy containment time assuming that the heat sources in the plasma and heat conduction coefficients are spatially constant. Then, one finds that the energy containment time is that in the absence of the island multiplied by $[1 - (w/a)(4r_s^3/a^3)]$. This formula gives roughly the right trend and, within a factor of about 2, roughly the right magnitude for the deterioration of confinement at low q that Mirnov discusses.

SLIDE #15 (DYNAMIC EVOLUTION OF MIRNOV OSCILLATIONS)

I want to emphasize the point that one must take account of the Mirnov oscillations and their implicit imposition of a magnetic island within the plasma and effect on the energy containment time, by showing results of some transport calculations done by John Hogan at Oak Ridge. Here, the current profile has been modified by neutral beam injection. He finds that the Mirnov Oscillation amplitude is significantly different with co-injection and counter-injection. The induced islands and their effects as illustrated at the top depend on the injection direction. In co-injection the islands move inward and that is the main reason why the amplitude of the Mirnov oscillation decreases with injection. In contrast, with counter-injection the current perturbation moves the islands outward and thereby produces a much larger magnitude of the Mirnov oscillations. These effects will greatly complicate trying to understand neutral beam injection experiments with large current perturbations, such are planned in ISX-B in the near future.

SLIDE #16 (DOUBLE TEARING MODE)

So far we have been discussing modes at one singular surface, and in particular m/n = 1 and 2. When one has a skin current, or in case two resonant surfaces occur within the plasma, one can have a double tearing mode that can lead to a skin current relaxation. The paper by Dnestrovskii et al. presents calculations of the early breakdown phases of a tokamak in which one expects to see a skin current effect. They begin by calculating the ionization stage. Basically they find that the time for breakdown and ionization of the plasma is about 2-4 msec and that the breakdown voltage required is about 50-100 volts -- in agreement with the T-10 experiments that they were modeling. They then find that the current profile at the end of the ionization stage is roughly bell-shaped or monotonic. That is, it has no skin current.

However, as one then heats beyond this 5-10 kA level one theoretically predicts that skin currents are produced. They propose that these skin currents

are relaxed by MHD mixing or magnetic reconnection during the current growth phase in the plasma -- that is, there is a skin current which leads to a double tearing mode which then leads to reconnection. The reconnection in this case is analogous to m = 1 internal disruptions; that is, it is a topological flip type of reconnection.

SLIDE #17 (KADOMTSEV MHD MIXING MODEL)

Dnestrovskii et al., utilize the Kadomtsev MHD mixing mode to calculate the reconnection process. That is, for a current profile as shown in the bottom diagram that has a skin current, one has two singular layers. From this current profile one calculates the helical flux function and reconnects (dashed line) the flux in such a way that the area occupied within any given amount of flux is always the same, as shown in the second diagram. The pitch profile and its reconnection (dashed line) are shown in the top diagram.

SLIDE #18 (m/n = 3 RECONNECTION PROCESS)

The dynamical evolution of this reconnection is illustrated by a calculation by Carreras et al. in Oak Ridge which show what happens for instance for an m = 3 mode. This particular case is for a hollow profile such as produced in ORMAK or PLT with substantial radiation from the plasma center. In the beginning or the early stages one can see m = 3 islands inside and outside, which are separated and not yet connected; however, as one goes on in time one finds that these island chains first intertwine and finally reconnect in such a way as to produce a new axisymmetric set of flux surfaces thereby having flattened the current profile over that region. One difference between the calculations in papers F-1-1 and F-1-3 is that Dnestrovskii reconnects whenever there is a skin current, whereas in paper F-1-1 it is found that most of the time the island chains separately saturate, and reconnection only occurs when the maximum of the helical flux function is equal to its value at the plasma center.

SLIDE #19 (RECONNECTION CAUSES EVOLUTION TO FLAT PROFILE)

Calculating this sort of process dynamically with the Kadomtsev flux mixing model in a transport code, Dnestrovskii et al. find that the reconnection produces a flat pitch or current profile. This is shown here where one begins with a relatively bell shaped current profile at 11 msec. Each time a skin current tries to form it gets flattened out by the relevant double tearing mode. Also shown in the dashed curve is what would happen if there were no MHD mixing or reconnection going on.

SLIDE #20 (CALCULATED CURRENT, VOLTAGE AND MAGNETIC ACTIVITY)

In addition, Dnestrovskii et al. make a more direct correlation of their theoretical calculations with experiment by showing this plot. Here, the calculated current, voltage and magnetic activity are shown during the current initiation phase in a tokamak. These results look very much like what one sees during the initial breakdown stages of a tokamak as the current rises. There, q at the limiter decreases through the rational numbers of 6, 5, 4, 3 and one sees correlated jumps in the voltage and magnetic activity.

SLIDE #21 (2/1-3/2 COUPLING)

Up to now we have been discussing modes of only one helicity. The next step is to consider what happens when we have modes of many helicities, or in particular incommensurate helicities. The evolution of such a case becomes our model of the disruptive instability. The basic mechanism is that when two modes which induce two island chains of incommensurate helicity overlap, they stimulate many other modes of different helicity and this leads to a destruction of the flux surfaces in the region of the plasma encompassed by the two original islands.

The mode coupling timescale for this process turns out to be governed by the linear growth of the 2/1 tearing mode.

This model of the disruptive instability is found to correlate with experimental observations in three important regards: 1) Negative voltage spike, because as we will show, the current channel is definitely broadened by virtue of the destruction of the flux surfaces; 2) Asymmetric evolution, i.e., up down asymmetry in the evolution, because of the 3/2 and 1/1 modes being strongly stimulated during the mode coupling process; and 3) The disruption timescale being on order of the 2/1 growth time, which as we will show does correlate with experimental observations.

SLIDE #22 (WHEN DOMINANT ISLANDS OVERLAP)

To demonstrate the basic mechanism, in this slide we show what happens when two growing modes get large enough for their associated magnetic islands to overlap. Specifically for the case where one has originally only the 2/1 and the 3/2 islands growing, one finds that many other islands are explosively excited at $t = 2 \times 10^3 \tau_{HP}$. Also shown is the current profile initially (t_1), next what it looks like at time t_2 where one is beginning to develop a little bit of a current broadening, and at time t_3 where one has very much broadened the current profile.

SLIDE #23 (FIELD LINES BECOME STOCHASTIC)

The magnetic field lines are becoming stochastic between times t_2 and t_3. At time t_2 one can see in the magnetic field structure the $m/n = 2/1$ and 3/2 islands quite easily. Some small 5/3 islands can also be seen here. Only 15% later in time when the islands have overlapped, one has produced totally stochastic field lines over the region encompassed by what one thinks would be the islands of one particular helicity. If the field lines were not stochastic the islands would be in the locations shown by the dashed lines.

SLIDE #24 (THEORETICAL TIMESCALE)

The theoretical timescale for the disruption is the 2/1 growth rate. This theoretical prediction is indeed found to correlate fairly well with experimental observations, to the best we can determine them at this time, of the disruption timescale, as shown in this graph. Here, the experimental timescale for the disruption is plotted against the theoretical estimate in dimensionless units. What one sees is a reasonably good correlation for a range of devices that runs from the small, relatively cold plasma in LT-3, all the way up to PLT -- a range of 2 orders of magnitude in the disruption time. Since γ_{21} is in fact the linear growth rate, it is somewhat surprising to see that it is the ultimate linear timescale. The reason it seems to true here is that for these large S values (up to 10^6 in the PLT case) the resistive flow mechanisms that usually slow up the growth of the tearing modes are in fact inhibited because the magnetic flux surfaces are destroyed.

SLIDE #25 (POSSIBILITY OF ISLAND OVERLAP)

The possibility of island overlap and hence disruptive instability is highest at the lowest q. Plotting the island width of the modes 2/1, 3/2 and 4/3 versus q at the limiter for a certain profile, we find that as q decreases the 2/1 island width grows. As we lower q still further the 2/1 mode dies down and then the 3/2 takes over and so forth. At the top of the figure we have plotted the singular radius and broadened it by approximately the island width as determined by these criteria. The net result of the nonlinear simulations has been to suggest that whenever these two islands of incommensurate helicity overlap, one gets a disruptive instability with the extent of the disruptive instability depending upon how far the islands extend just before they overlap. In the case shown the 2/1 and 3/2 islands do not quite overlap and there would not be a

disruptive instability. However, for a slight change in the current profile, namely by increasing the current gradients at the 2/1 and 3/2 singular surfaces, one would get overlapping islands and hence a disruptive instability. One may be able to sneak down to a relatively low value of q at the limiter if one adjusts the current profile. In the case shown when one gets down to a q of about 1.6 it looks like the 3/2 and 4/3 islands would overlap and induce a disruptive instability.

SLIDE #26 (FEEDBACK CONTROL OF 2/1 MODE)

The primary mechanism for preventing the disruptive instability is to control the magnitude of the 2/1 mode, since it is the largest and most externally accessible mode. We have done some calculations of feedback control of the 2/1 mode. Basically what we find is that indeed at least for some fairly short feedback response times ($\ll\gamma_{21}^{-1}$) the amplitude of the 2/1 mode can be kept to a fairly small value.

SLIDE #27 (HIGH MODE NUMBERS)

As we have discussed earlier, the investigation of the temperature perturbation induced by the internal disruptions shows that the anomalous electron heat transport in tokamaks is a diffusive and fairly microscopic process. Thus, in anology with the effects of low mode numbers, we discuss the effects of high mode number magnetic perturbations -- in order to see if they can explain the microscopic anomalous transport. In general the consideration of microscopic magnetic turbulence is an alternative to the usual anomalous transport models that consider the effects of electrostatic turbulence.

The basic microscopic modes are the drift and shear-Alfvén modes. These modes are both unstable in a local theory, with or without the inclusion of trapped particle effects. When shear is included, we have found, contrary to

the Pearlstein-Berk theory, that the collisionless modes of both types are stable. When trapped particle effects are included these modes become unstable in a linear theory. The question mark is added here because the theory of such modes is currently being reexamined because of the fact that the present theory includes some seemingly unphysical singularities in it. Both types of microinstabilities have magnetic perturbations that indeed could induce microscopic magnetic islands.

Microscopic magnetic islands can grow and have the same effects as we have been discussing for the macroscopic modes. While a complete nonlinear theory has not yet been developed, the generic consequences of magnetic perturbations is fairly clear. Namely, since the electrons would diffuse radially very rapidly they cause the buildup of an ambipolar potential to confine the electrons electrostatically. The ambipolar potential would not effect runaway electrons, so one would expect that runaway or pullaway electrons would have a containment time comparable to the overall plasma energy containment time. Further, one would expect electron temperature fluctuations to be larger than density fluctuations, because of the radial extent of the islated and/or stochastic field line structures. Finally, since electrons would diffuse radially by their very rapid motion along the wobbling field lines one would expect electron heat conduction to be the dominant nonradiative loss process in tokamaks. While the "magnetic flutter" models of anomalous transport process have not yet yielded a correct formula for the electron energy containment time, since most of these generic consequences are observed in tokamak experiments we are encouraged that they may hold the key to resolving this major enigma of tokamak plasma confinement.

SLIDE #28 (SUMMARY)

In summary tokamak discharge behavior seems to be beginning to be understandable and even calculable in terms of the collective magnetic perturbation effects in tokamaks. In a typical tokamak discharge as shown one sees various stages. During the current rise (stage 1) the voltage decreases with some little steps in it. Correlated with this are magnetic ($\tilde{B}_\theta$) perturbations with m = 6, 5, 4, 3, and then finally a steady m = 2 mode. During the current initiation phase (1) , it seems that one has successive double tearing mode relaxations -- or MHD mixing as Kadomtsev would say -- of the skin current.

In the quasi-equilibrium or second stage one can have: 1) internal disruptions, which don't effect energy containment too much; 2) Mirnov oscillations as evidenced by the external magnetic loop measurements and having a minor effect on energy containment except at small q; 3) soft disruptions due to hollow profiles causing double tearing modes; and 4) anomalous transport due to very high mode number microscopic magnetics. One of the most important things to realize out of all these possibilities is that, as emphasized by Mirnov in his paper F-1-2 being rapporteured here, in determining transport scaling laws, one must systematically remove all of the MHD effects to obtain a true transport scaling law. Otherwise the MHD effects can effectively obscure the scaling of the miroscopic transport processes. Finally, an abnormal discharge termination commonly referred to as a disruptive instability can occur whenever one has tearing modes of incommensurate helicity that grow up and overlap and thereby produce large stochastic field regions.

TOKAMAK DISCHARGE MODELING THROUGH MAGNETIC PERTURBATION EFFECTS

F-1-1 Magnetic "Islandography" in Tokamaks (J. D. Callen, et al.)

- m/n = 1: internal disruptions
- m/n = 2: Mirnov oscillations
- 2/1 - 3/2 coupling: disruptive instability
- Microinstabilities ($\tilde{\underline{B}}$): anomalous transport

F-1-2 Scaling Laws for Energy Lifetimes in Tokamaks (S. V. Mirnov)

- Universal scaling of τ_E with $q(a_I)$
  - -- correlation with Mirnov oscillations
- Confinement scaling law: $\tau_E \sim aI/\bar{n}_e$

F-1-3 Simulation of Discharge Dynamics in Tokamaks (Yu. N. Dnestrovskii, et al.)

- Skin current relaxation through magnetic reconnection
- Neutral beam heating in T-11

FED/VU 78-157

500-kW NEUTRAL BEAM HEATING IN T-11; COLLISIONLESS REGIME ($\nu_{*_i} < 1$) ACCESSIBLE IF $Z_{EFF} < 4$-5, $N_0 < 1.5 \times 10^{10}$

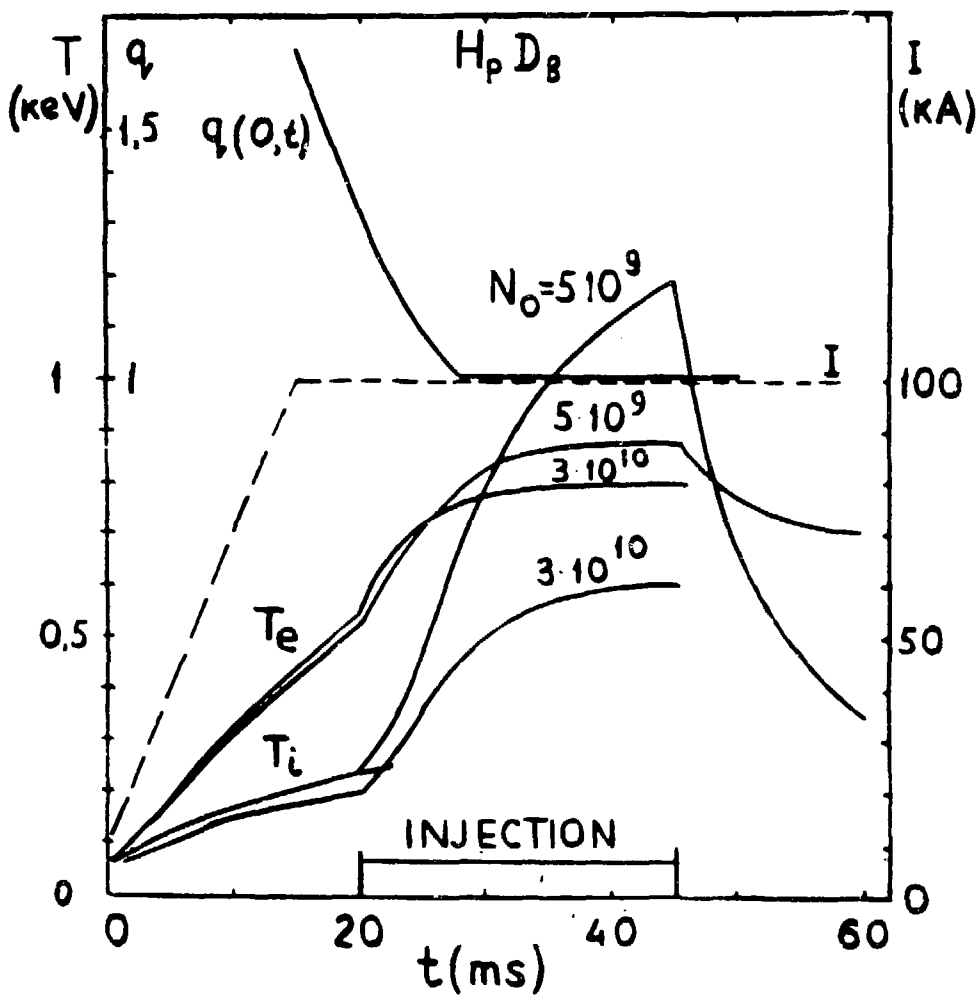

F–1–3

NONLINEAR EVOLUTION OF MAGNETIC PERTURBATIONS AND THEIR EFFECT ON TRANSPORT

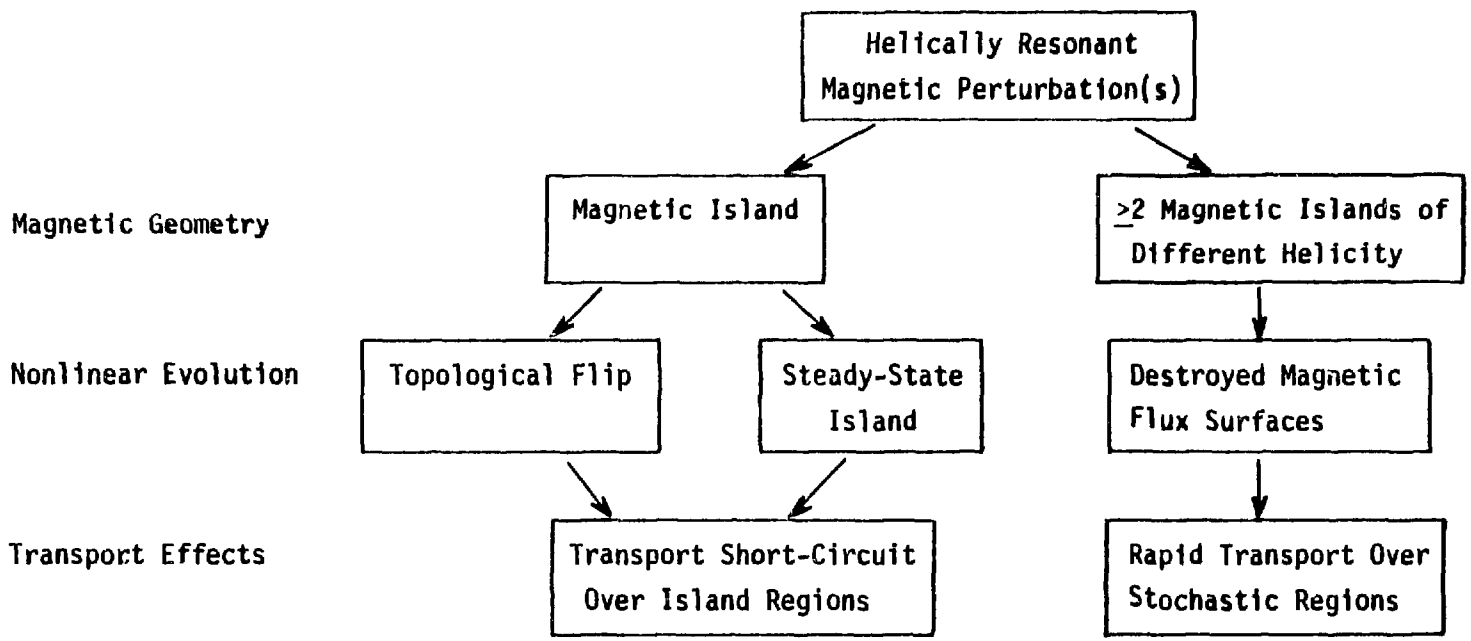

F-1-1

ORNL/DWG/FED 78-788

m/n = 1 — INTERNAL DISRUPTIONS

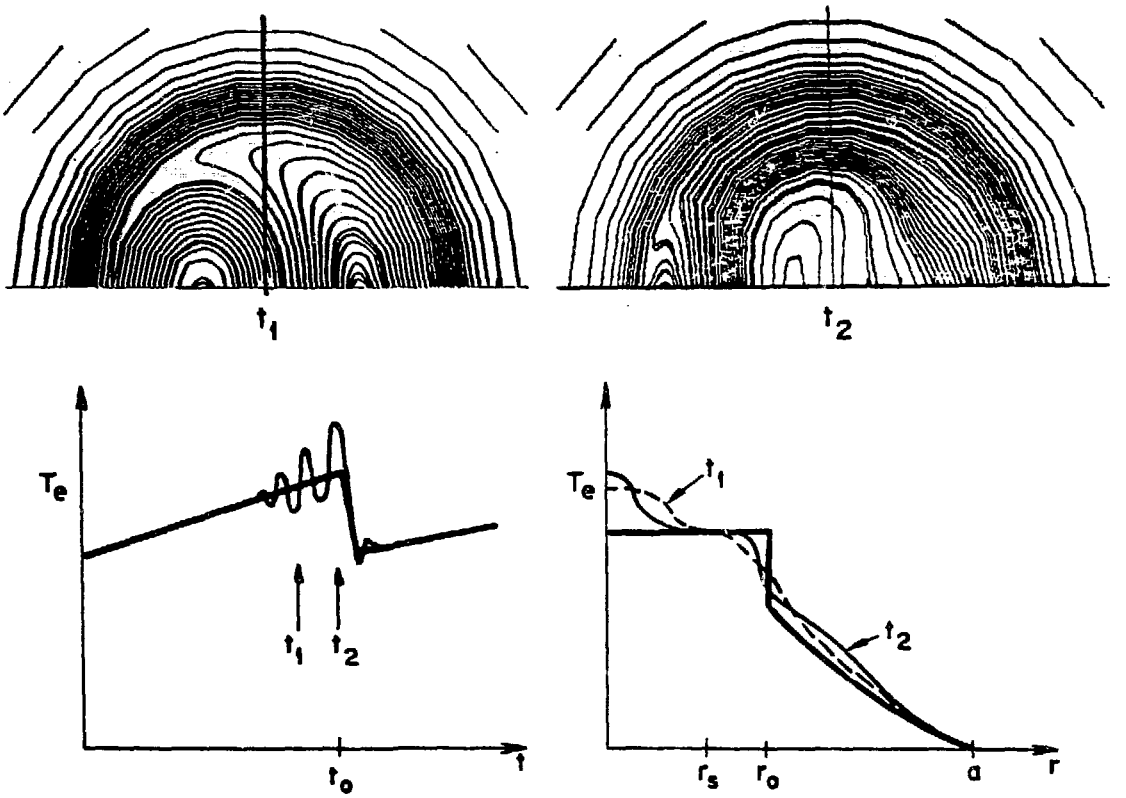

MODEL AGREES WITH ORMAK DATA IN:

1) SPACE-TIME EVOLUTION OF m = 1 PRECURSORS
2) INTERNAL DISRUPTION TIME t_0 AND SPATIAL STRUCTURE
3) HEAT PULSE PROPAGATION – MICROSCOPIC DIFFUSIVE PROCESS

ELECTRON HEAT TRANSPORT DETERMINATION IN ORMAK FROM HEAT PULSE PROPAGATION:

- DIFFUSIVE, MICROSCOPIC (<1-2 cm) PROCESS
- SAME CONDUCTION COEFFICIENT AS PLASMA

ORNL/DWG/FED 77-1020A

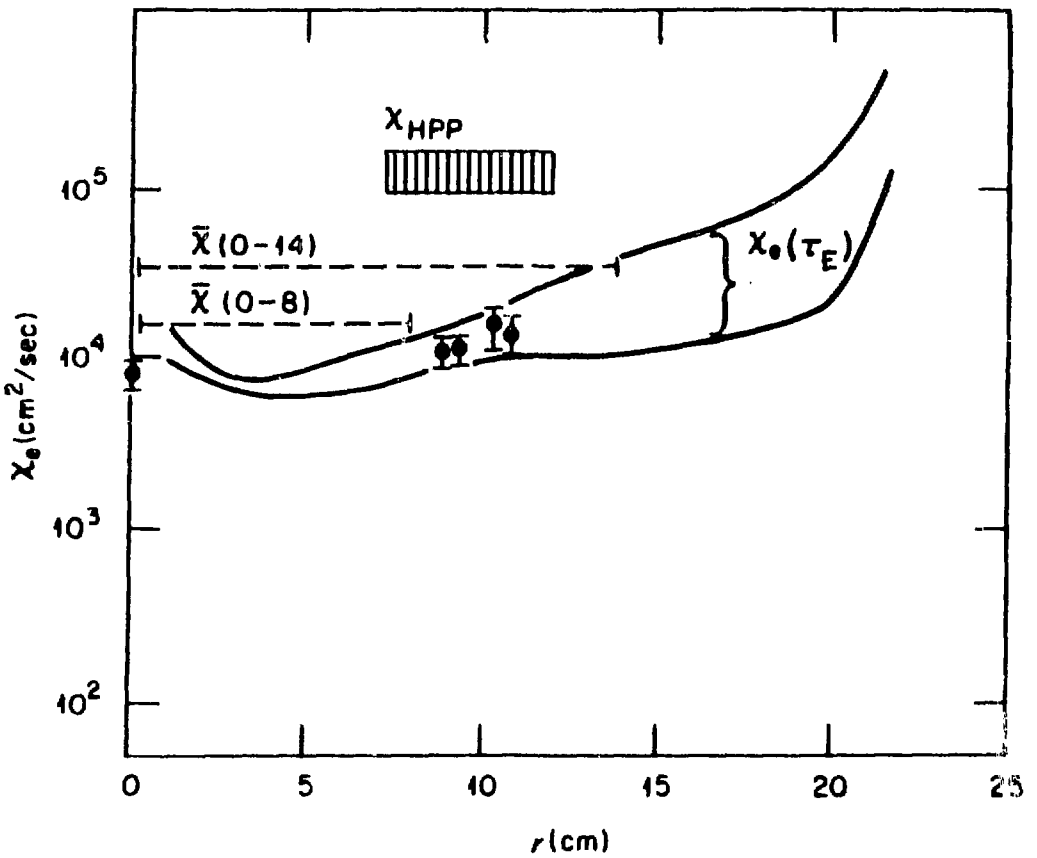

F-1-1

5

M/N = 2 -- MIRNOV OSCILLATIONS

- Nonlinear Evolution:

$$\frac{dw}{dt} \sim \eta \Delta'(w)$$

$$w = \text{island width} \sim \tilde{B}_r^{1/2}$$

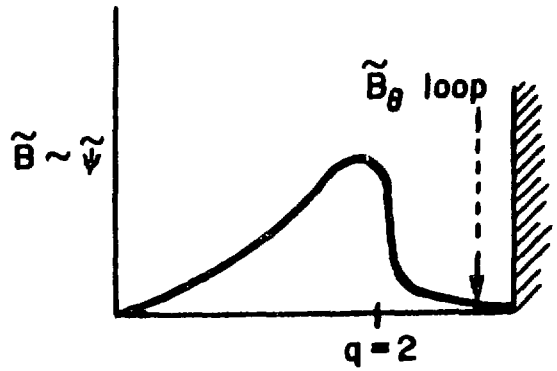

- Quasilinear Saturation:

$$\Delta'(w_{max}) \simeq 0 \rightarrow w_{max} \rightarrow \tilde{B}_\theta \text{ at loops}$$

- Theoretical Prediction of $\tilde{B}_\theta$ Compares Favorably With ORMAK and T-4 Data

ORNL/DWG/FED 78-785

THEORETICAL MIRNOV OSCILLATION AMPLITUDE AND 2/1 ISLAND WIDTH PEAK AT $q(a) \lesssim 3$

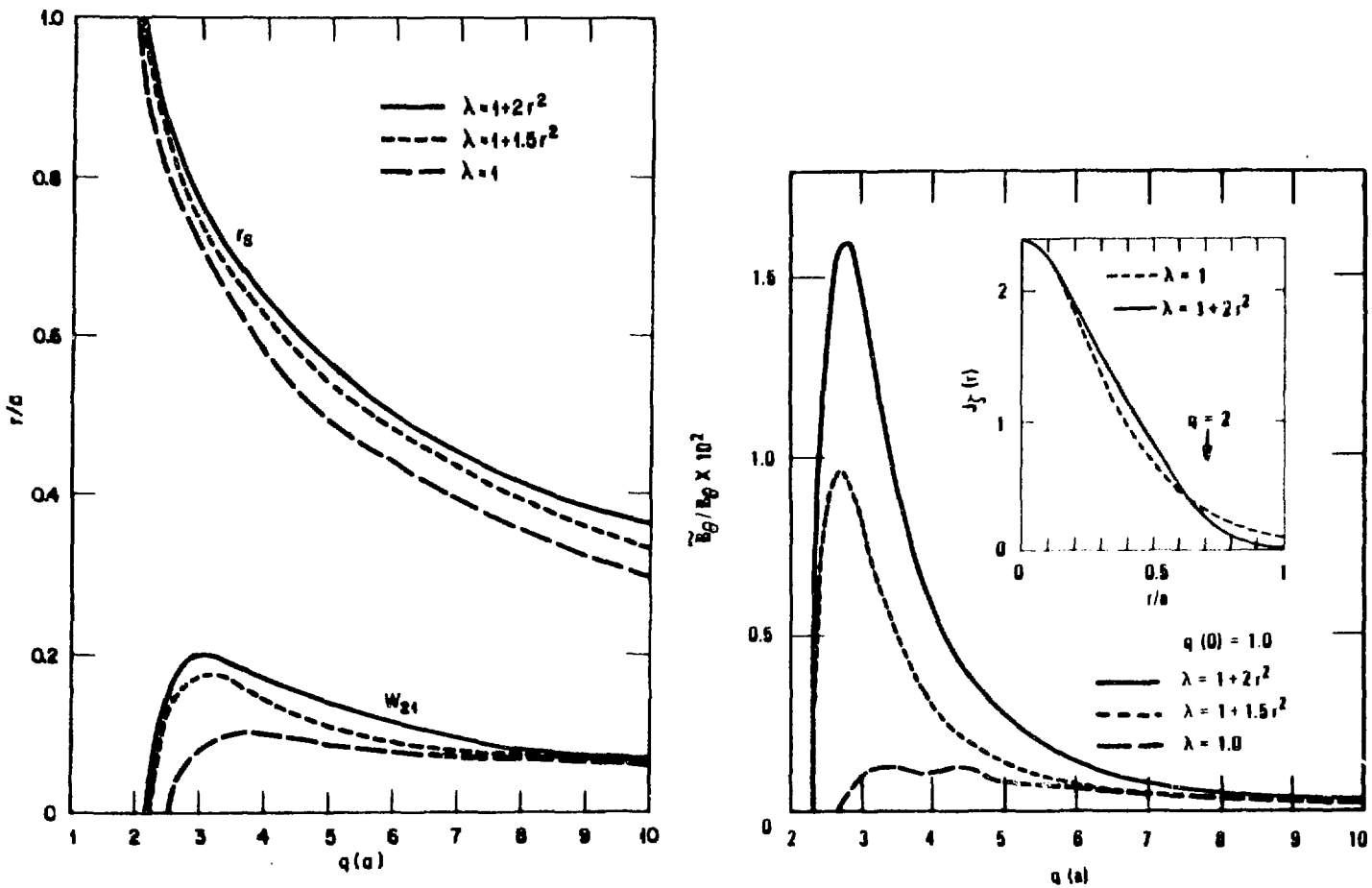

F-1-1

7

8

THEORETICAL MIRNOV OSCILLATION AMPLITUDE AGREES WITH ORMAK DATA

ORNL/DWG/FED 78-130R2A

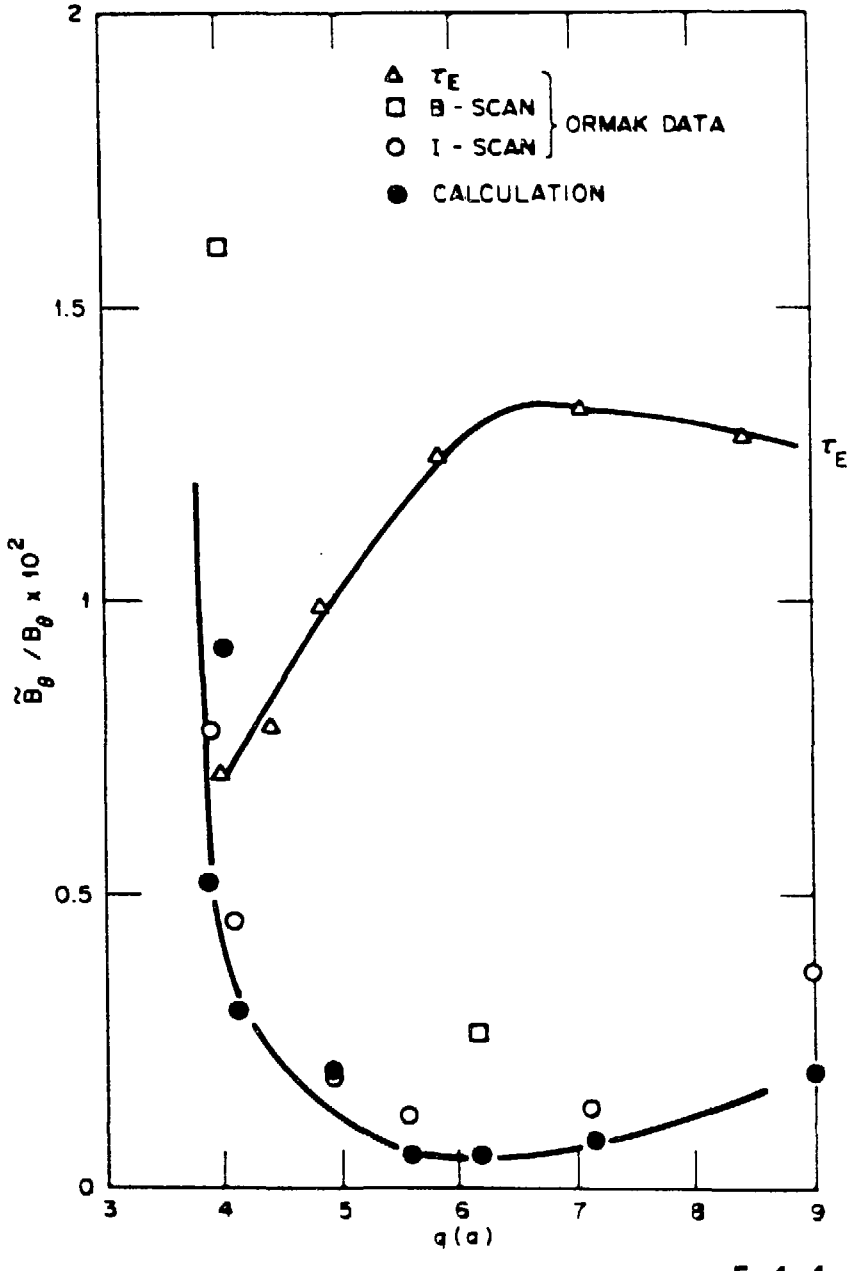

F-1-1

ENERGY CONTAINMENT TIME CORRELATED WITH MIRNOV OSCILLATION AMPLITUDE IN T-4 (I) AND ORMAK (II) —BUT PEAK CONFINEMENT OCCURS AT DIFFERENT q(a)

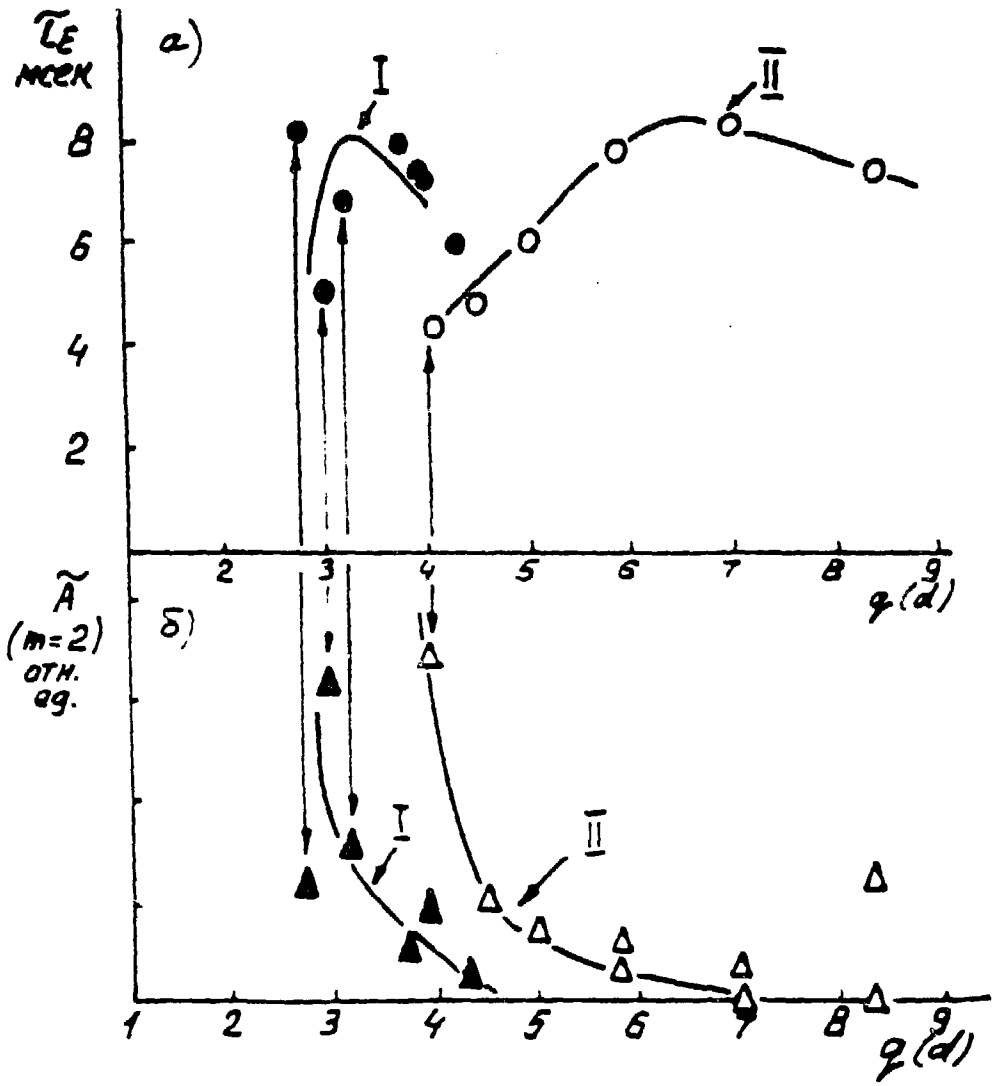

Рис 2

MIRNOV RECONCILES DIFFERENCE IN τ_E PEAK LOCATION BY TAKING ACCOUNT OF CURRENTLESS COLD PLASMA MANTLE

- Current Channel Radius Determined From:

  Mean radius of resonant surface: $q(a_I) = 2 \rightarrow a_I = \sqrt{\frac{0.4IR}{B_Z}}$

  Electron temperature profile: $T_e(a_I) = 0.1\ T_e(0)$

- Thickness of Currentless Cold Plasma Region:

  $\delta = a - a_I$ -- governed by experimental conditions

- Relevant q Is That at Current Channel Radius:

  $q(a_I) = (a_I/a)^2\ q(a)$

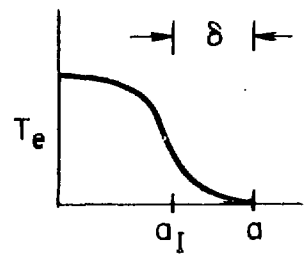

F-1-2

RENORMALIZING THE q AXIS TO q AT CURRENT CHANNEL RADIUS RESULTS IN UNIVERSAL SCALING CURVE OF τ_E VS $q(a_I)$

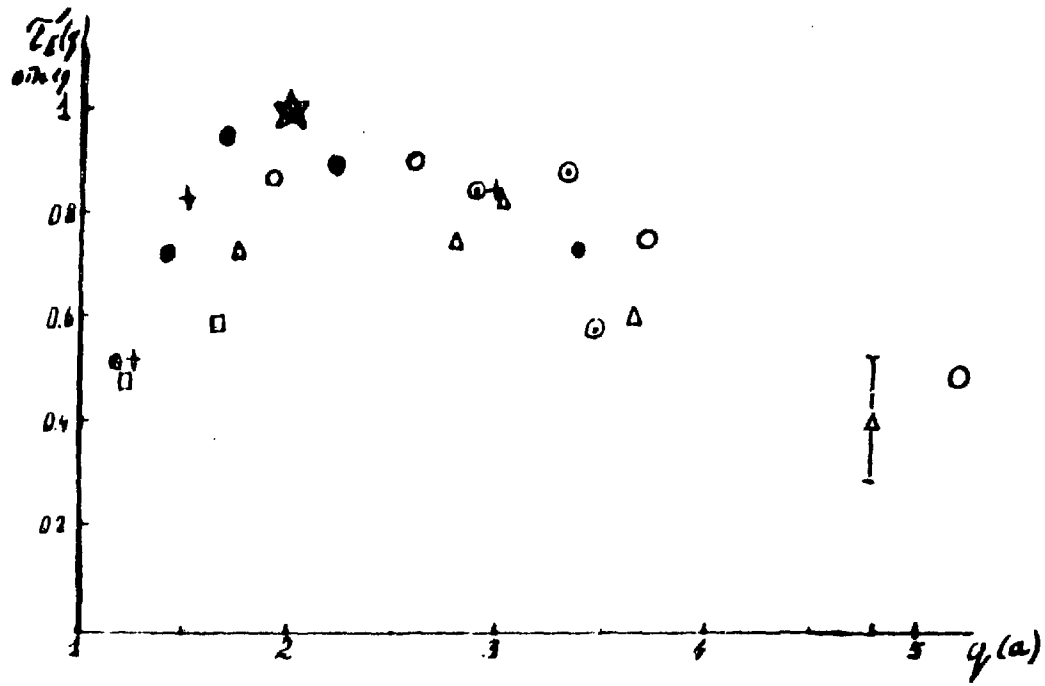

Рис 5

FED/VU 78-152

T-3 SCALING LAW FITS TOKAMAK DATA BETTER THAN ALCATOR SCALING LAW FOR STABLE DISCHARGES

$$\left[q(a^0) \geq 2,\ q(a) > 4\text{-}6\right]$$

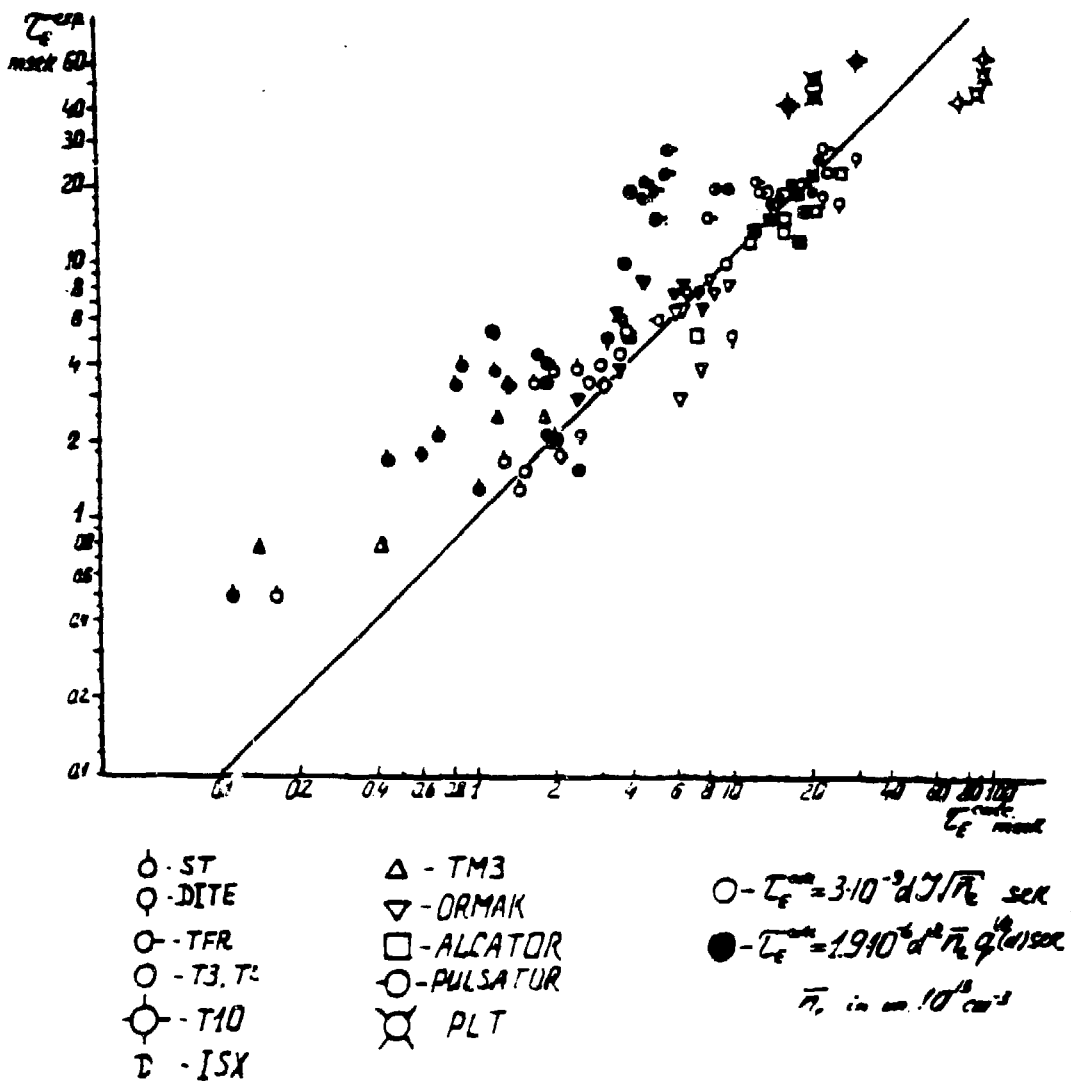

F–1–2

FED/VU 78 - 153

CONFINEMENT DETERIORATES FOR "UNSTABLE" DISCHARGES

$\left[q(a^0) < 2,\ q(a) < 4\text{-}6\right]$

—BUT MAY IMPROVE FOR $q(a) < 2\text{-}3$

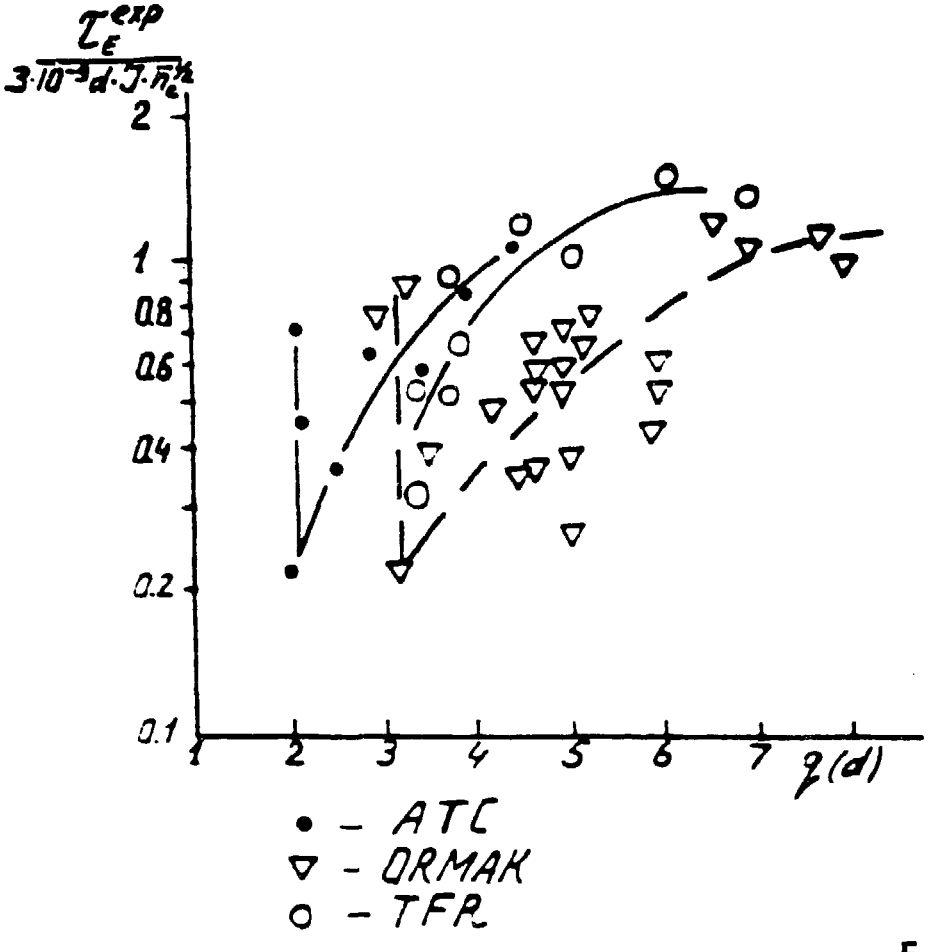

F–1–2

PLASMA CONFINEMENT DETERIORATES AT LOW q DUE TO MIRNOV OSCILLATION-INDUCED MAGNETIC ISLAND

- HELICAL FLUX SURFACE GEOMETRY
- TRANSPORT SHORT CIRCUIT
- $\tau_E \sim \tau_{E_0} [1-(w/a)(4r_s^3/a^3)]$

ORNL/DWG/FED 78-732A

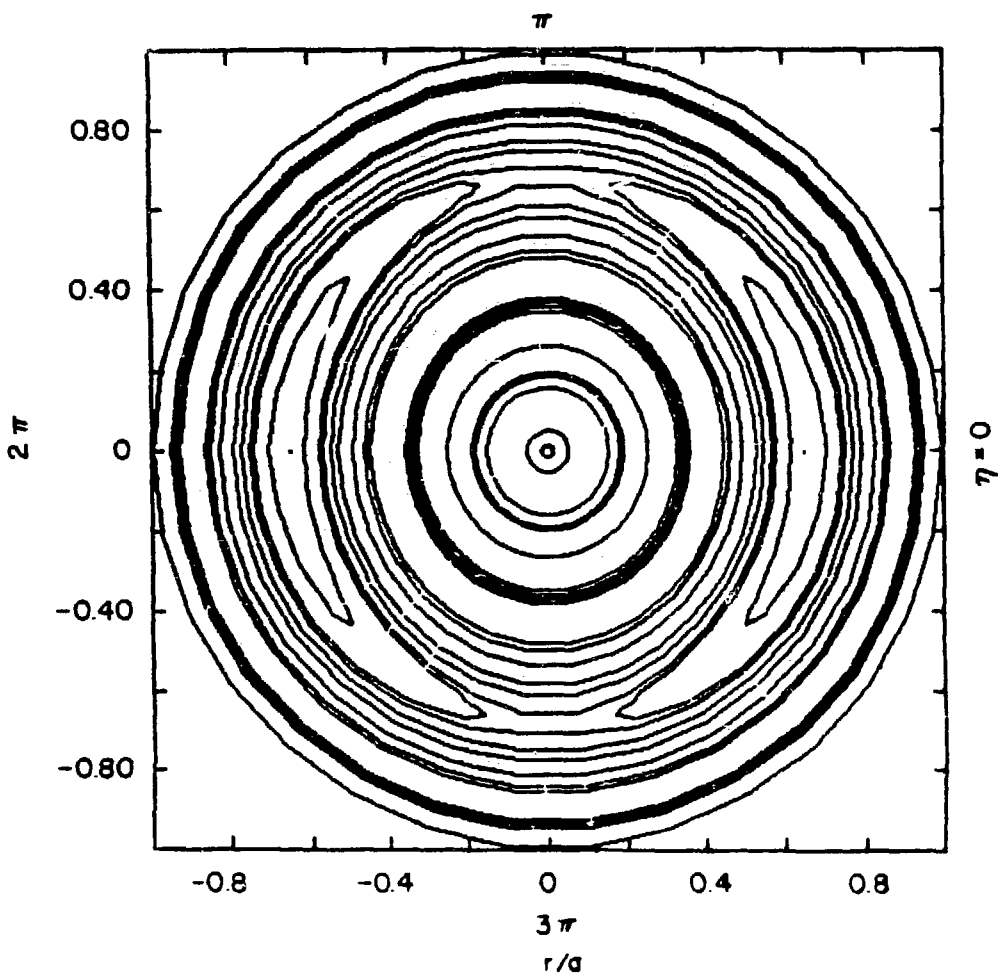

F-1-1

ORNL/DWG/FED 78-787

DYNAMIC EVOLUTION OF MIRNOV OSCILLATIONS CAN COMPLICATE ANALYSIS OF NEUTRAL BEAM HEATING EXPERIMENTS WITH LARGE $\Delta I/I$ (J. T. HOGAN)

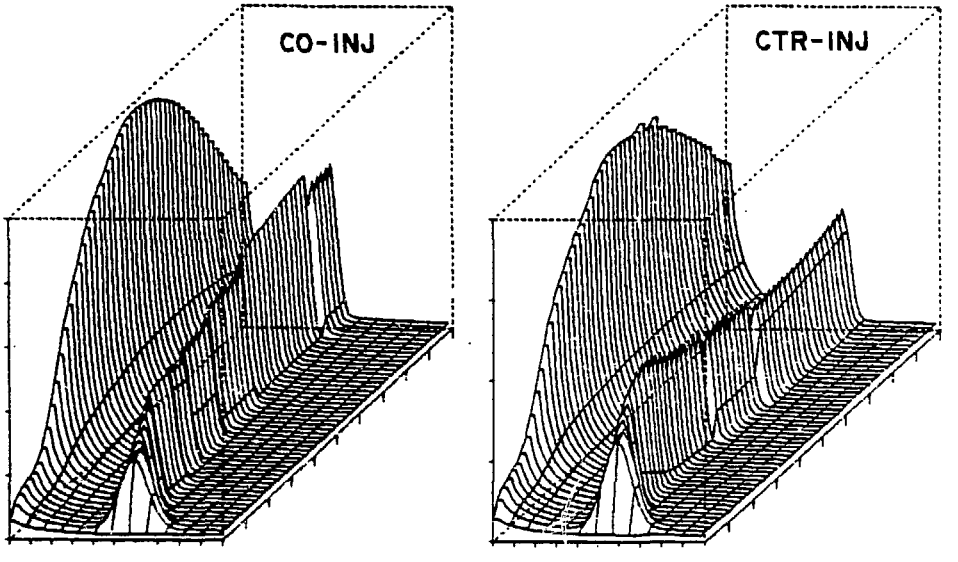

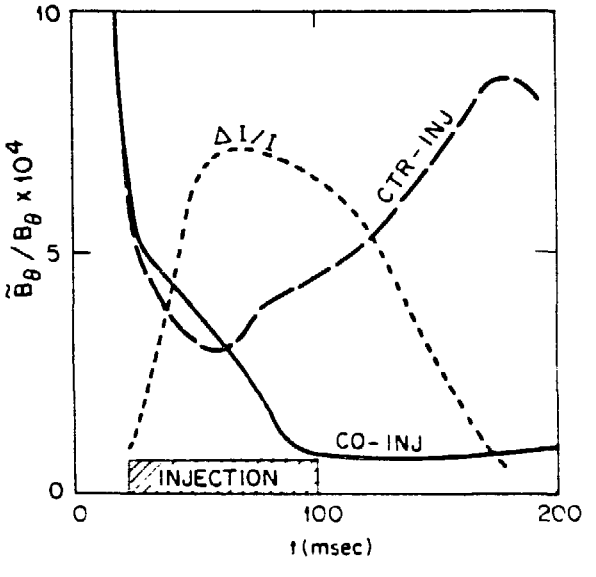

F-1-1

DOUBLE TEARING MODE -- SKIN CURRENT RELAXATION

- Ionization Stage Calculated:

  $\tau^i \sim$ 2-4 msec, $U_B \sim$ 50-100 V

  Bell-shaped current profile

- MHD-Mixing (Reconnection) During Current Growth Phase

  Skin current → Double tearing mode → Reconnection

  Reconnection analogous to m = 1 internal disruption

FED/VU 78-156

KADOMTSEV MHD MIXING MODEL USED TO CALCULATE RECONNECTION PROCESS

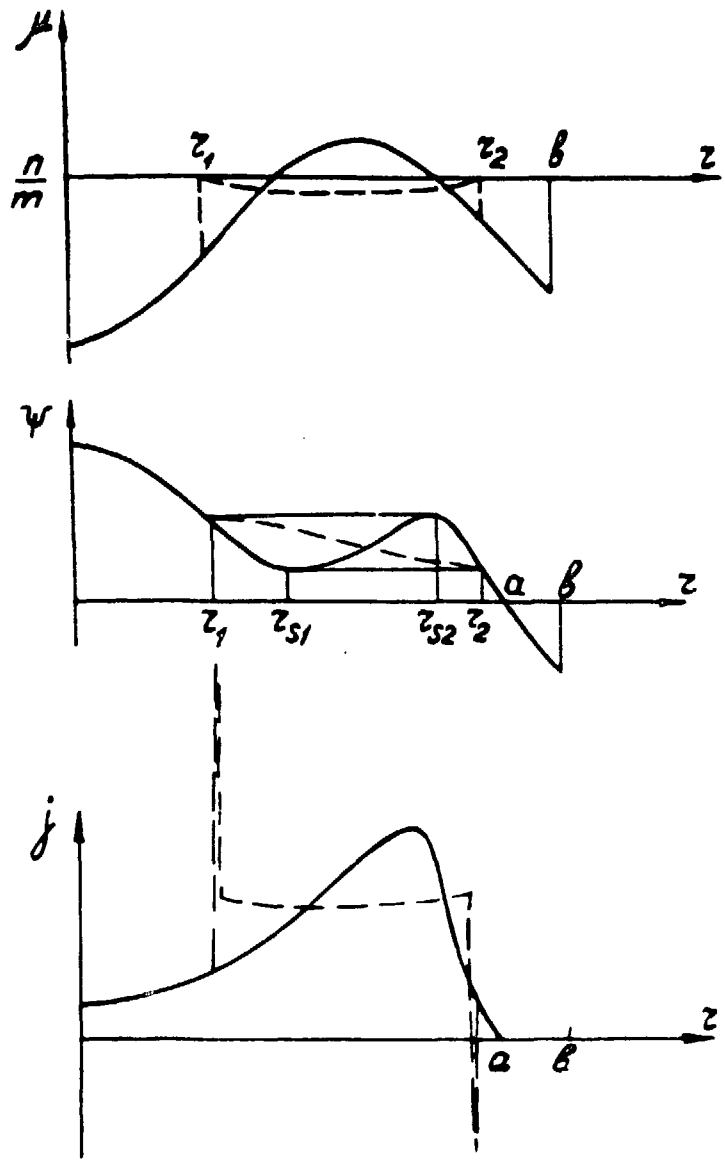

F-1-3

m/n = 3 RECONNECTION PROCESS SIMILAR TO INTERNAL DISRUPTION

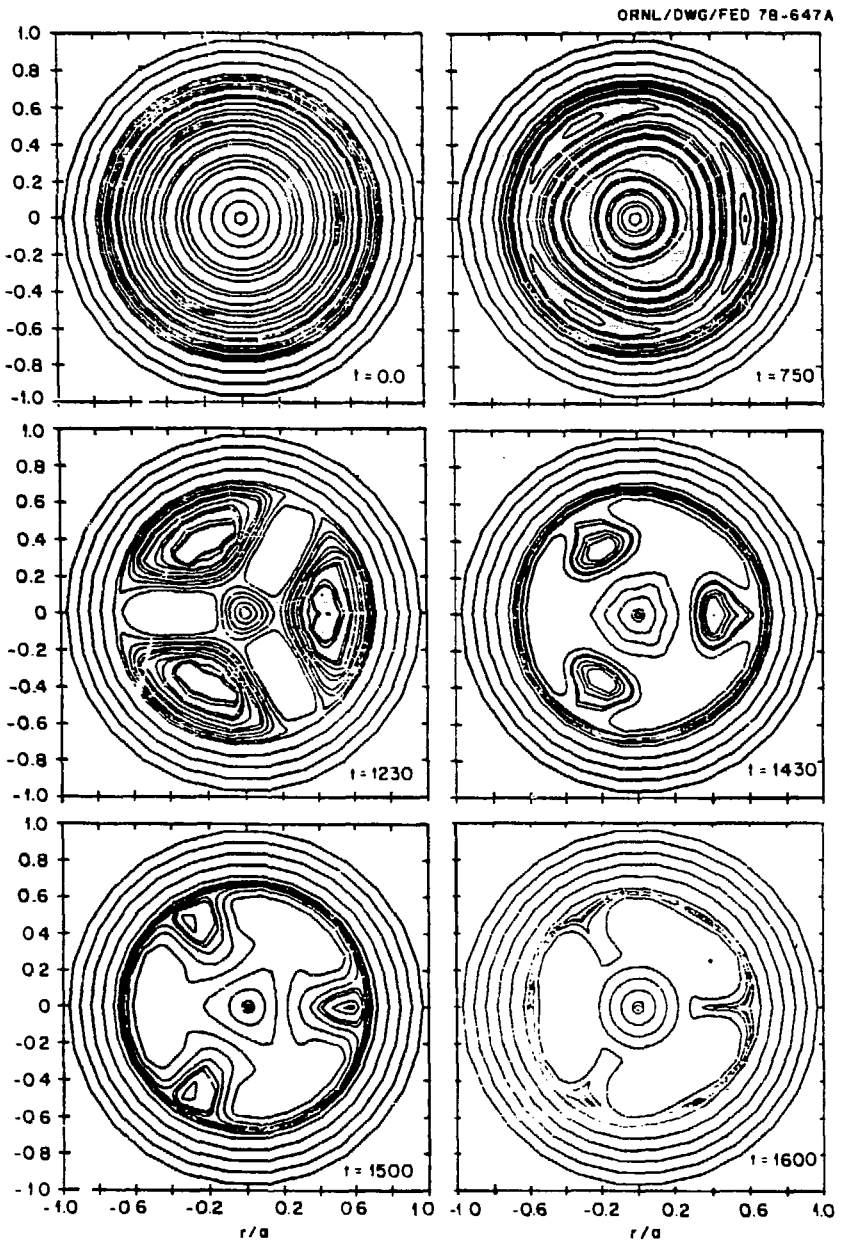

F–1–1

FED/VU 78-159

RECONNECTION CAUSES EVOLUTION TO FLAT PITCH PROFILE
—INCLUDE IMPURITY RADIATION AS WELL FOR PEAKED PROFILE

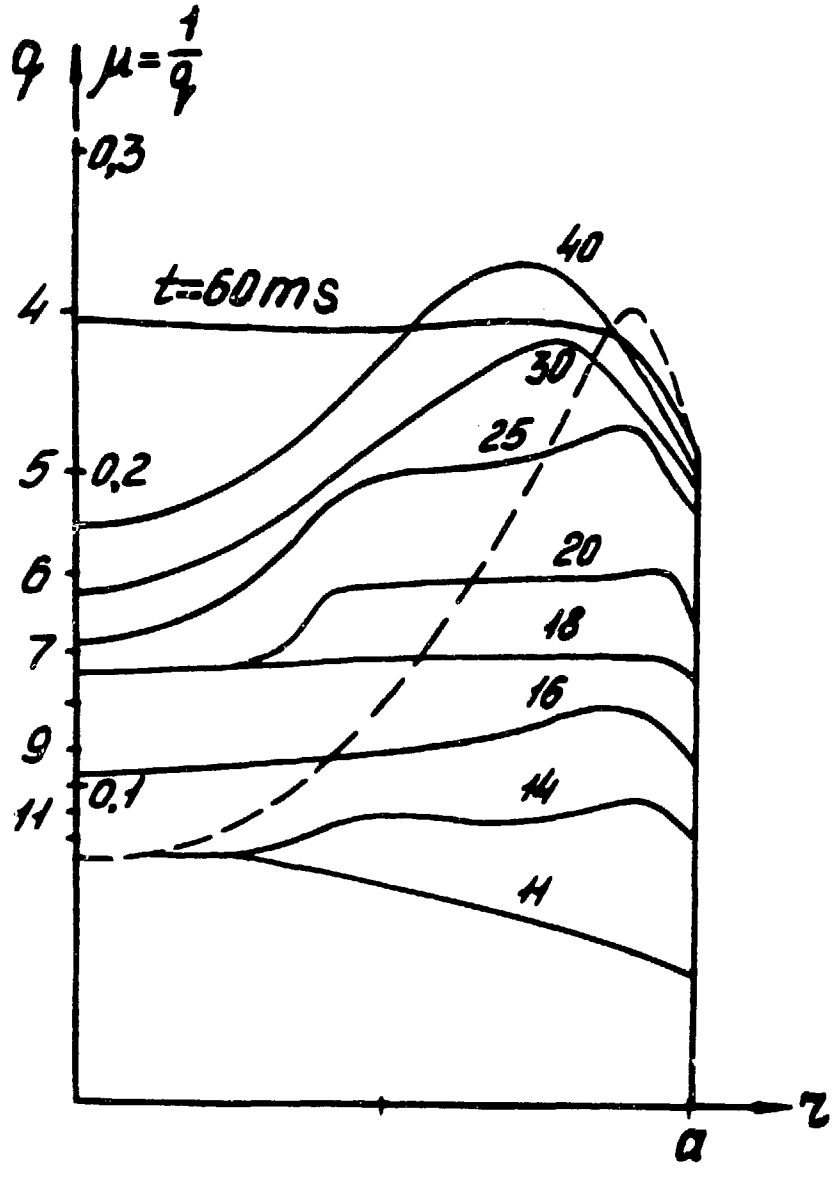

F–1–3

FED/VU 78-154

CALCULATED CURRENT, VOLTAGE, AND MAGNETIC ACTIVITY CORRELATE WELL WITH OBSERVED TOKAMAK DISCHARGE BEHAVIOR IN CURRENT INITIATION PHASE

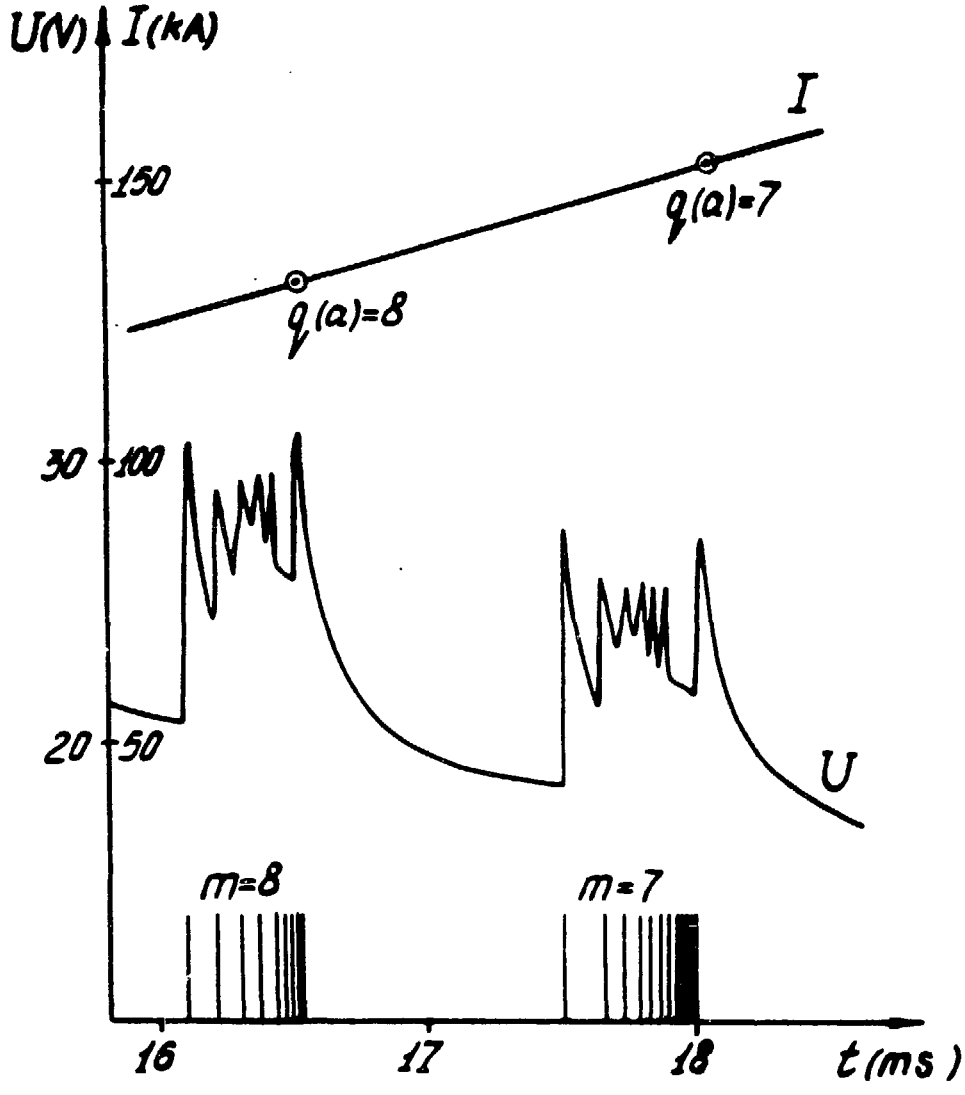

F-1-3

2/1 - 3/2 COUPLING -- DISRUPTIVE INSTABILITY

- Basic Mechanism:

  2/1 - 3/2 Island overlap → stimulation of other modes → destruction of flux surfaces

- Mode-Coupling Time Scale Governed by Linear Growth Rate of 2/1 Tearing Mode

- Model Correlates with Experimental Observations

  Negative voltage spike -- current channel broadened

  Asymmetric evolution -- 1/1, 3/2 modes stimulated

  Time scale -- $\Gamma \sim \gamma_{21}^{-1} \sim \tau_R^{3/5} \tau_{Hp}^{2/5}$

ORNL/DWG/FED 78-786

WHEN DOMINANT ISLANDS OVERLAP, OTHER ISLANDS EXPLOSIVELY ($\Delta t \sim \gamma_{21}^{-1}$) EXCITED AND CURRENT PROFILE DEFORMED ($S = 10^6$)

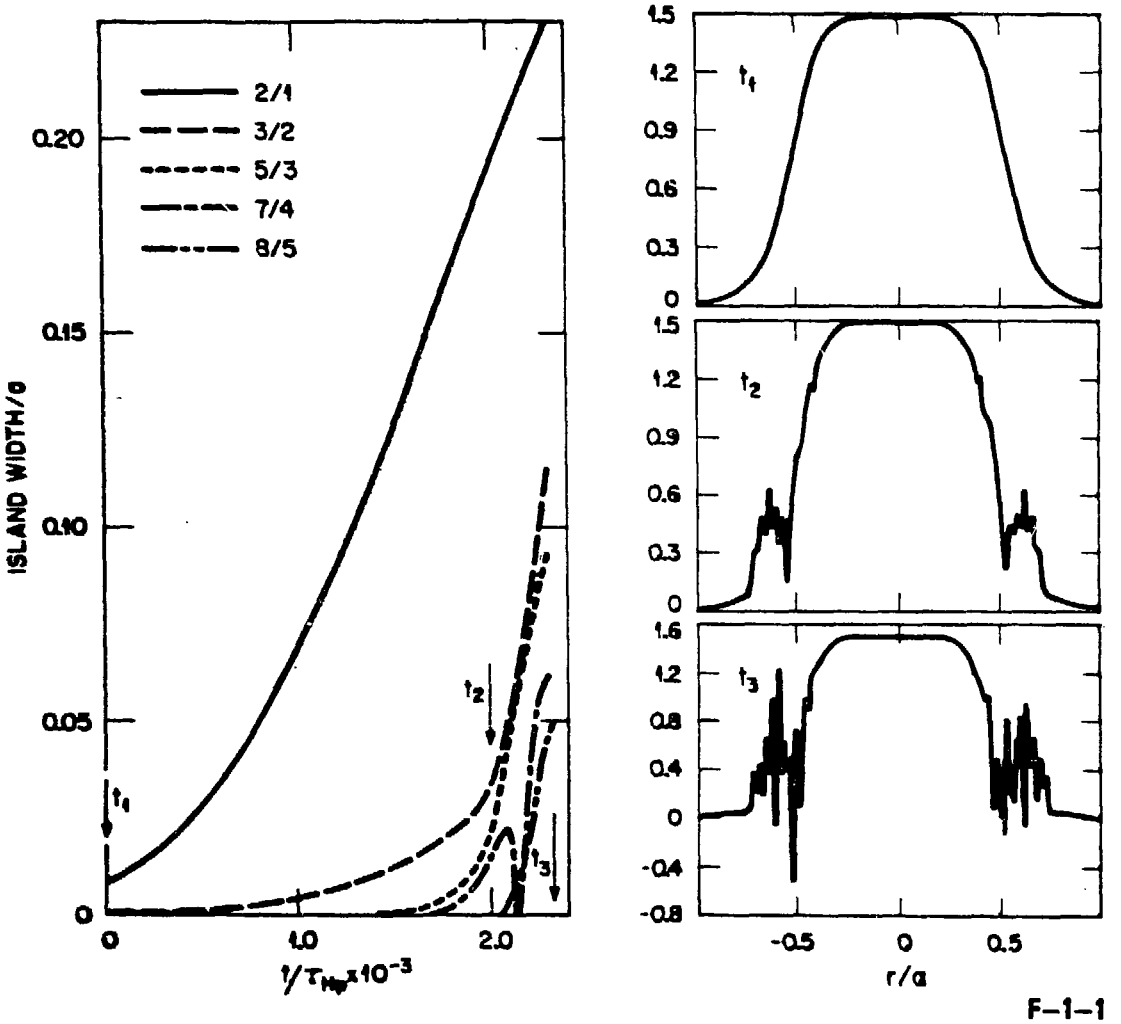

F-1-1

ORNL/DWG/FED 78-606A2

FIELD LINES BECOME STOCHASTIC WHEN ISLANDS OVERLAP

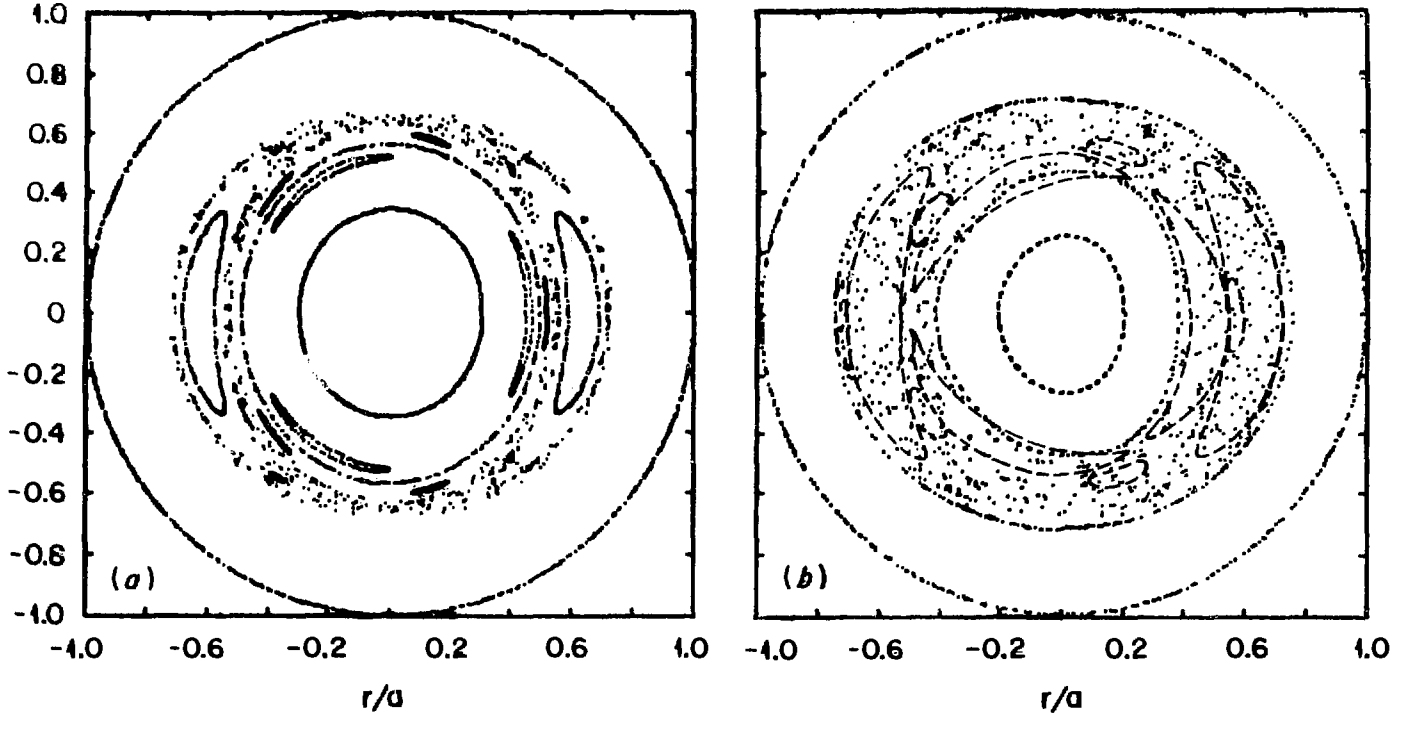

F-1-1

23

THEORETICAL TIME SCALE FOR DISRUPTION ($\Gamma \sim \gamma_{21}^{-1} \sim \tau_R^{3/5} \tau_{Hp}^{2/5}$) CORRELATES WELL WITH EXPERIMENTAL OBSERVATIONS

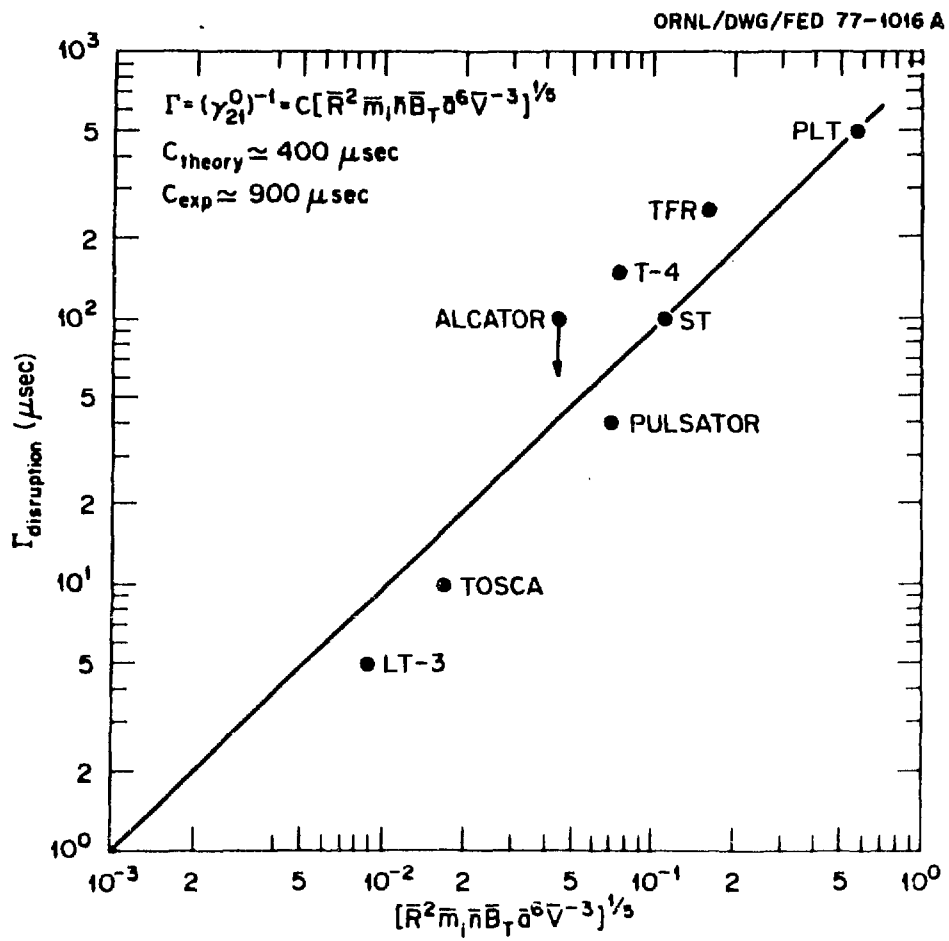

F-1-1

24

POSSIBILITY OF ISLAND OVERLAP AND HENCE DISRUPTIVE INSTABILITY HIGHEST AT LOW q(a)— PROFILE DEPENDENT

ORNL/DWG/FED-78-761A

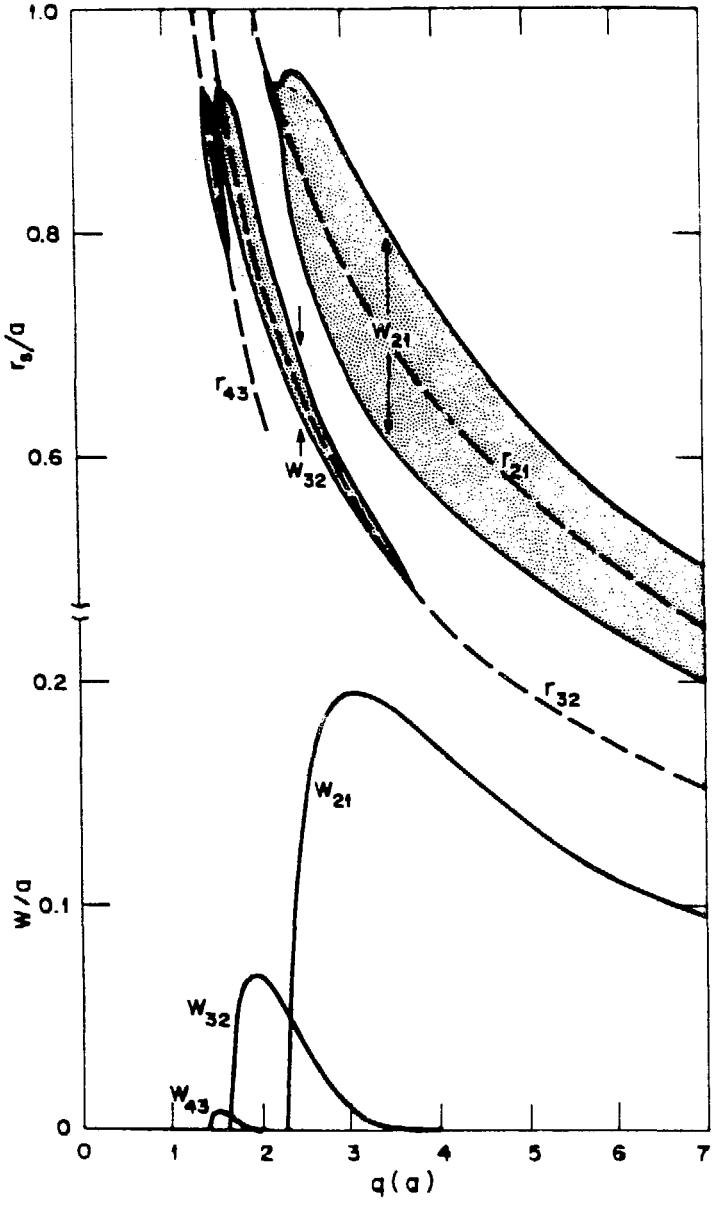

F-1-1

FEEDBACK CONTROL OF 2/1 MODE POSSIBLE IF RESPONSE TIMES SHORT ENOUGH ($\ll \gamma_{21}^{-1}$)

ORNL/DWG/FED 78-763A

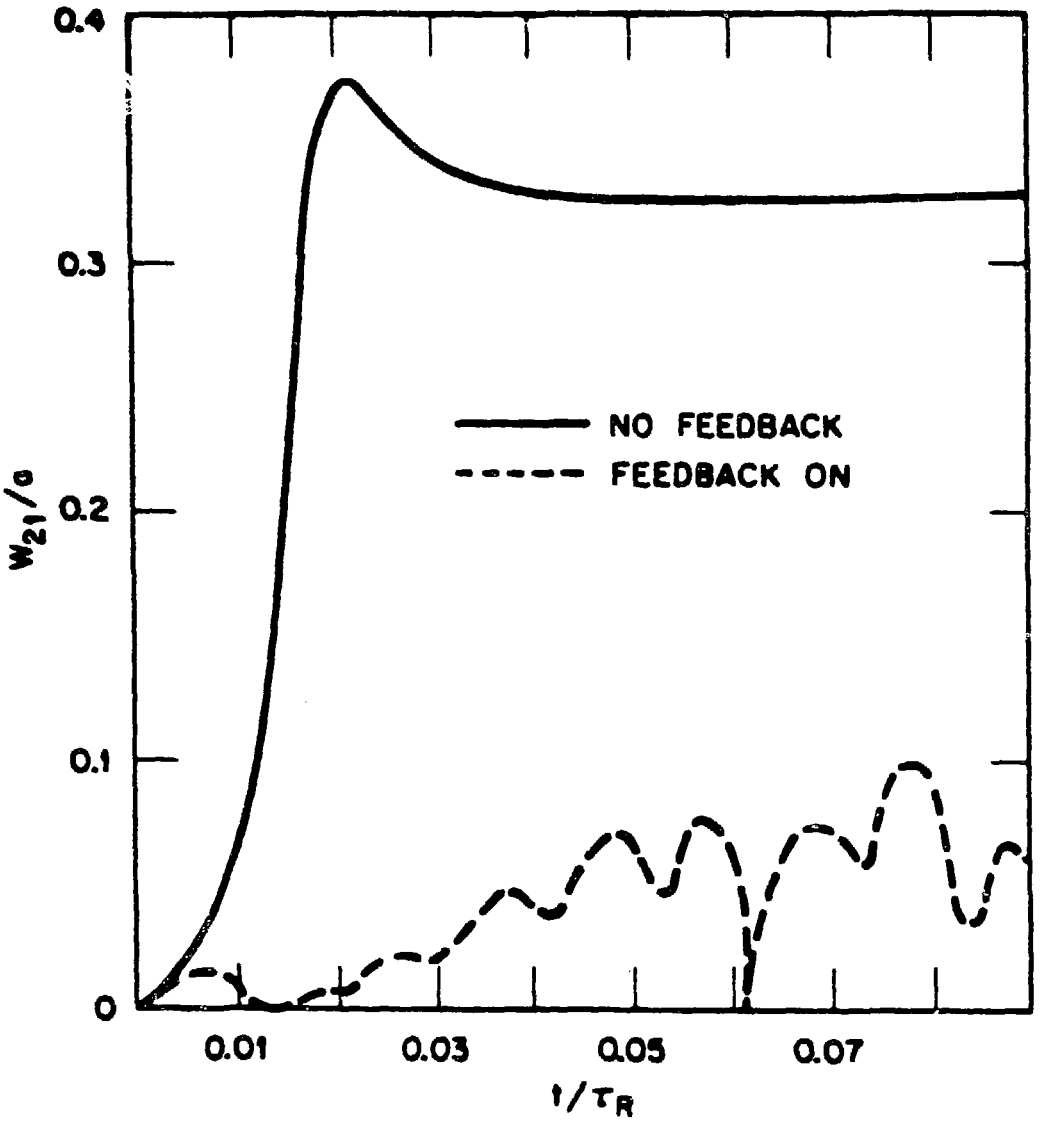

F-1-1

HIGH MODE NUMBERS -- MICROSCOPIC ANOMALOUS TRANSPORT?

- Magnetic Microturbulence -- Alternative to Electrostatic Turbulence

- Finite β Microinstabilities:

	local theory	with shear
Collisionless drift	unstable	damped
Collisionless shear-Alfvén	unstable	damped
Trapped-particle drift	unstable	unstable
Trapped-particle shear-Alfvén	unstable	unstable?

- Generic Consequences of "Magnetic Flutter" Transport Models:

  Ambipolar potential -- confinement electrostatically
  Runaway electron confinement time $\tau_R \approx \tau_E$
  Temperature fluctuations larger than density fluctuations
  Electron heat conduction dominant nonradiative loss

SUMMARY: TOKAMAK DISCHARGE BEHAVIOR

UNDERSTANDABLE AND MOSTLY CALCULABLE

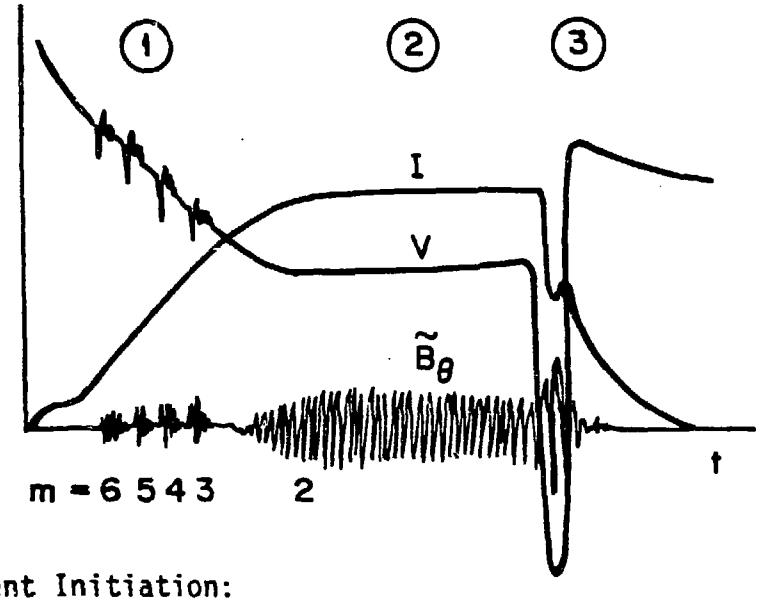

(1) Current Initiation:

Double tearing mode relaxation of skin current

(2) Quasi-Equilibrium:

Internal disruptions (m/n = 1)
Mirnov oscillations (m/n = 2,3,...)
Soft disruptions (double tearing modes)
Anomalous transport (m,n >> 1)
Transport scaling laws -- take out MHD effects

(3) Abnormal discharge termination:

Disruptive instability (2/1-3/2 coupling)